Chemical Engineering Journal 425 (2021) 130538

Contents lists available at ScienceDirect

Chemical Engineering Journal

journal homepage: www.elsevier.com/locate/cej

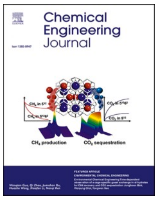

Designing a simple volumetric apparatus for measuring gas adsorption equilibria and kinetics of sorption. Application and validation for CO_2, CH_4 and N_2 adsorption in binder-free beads of 4A zeolite

Mohsen Karimi [a,b,*], Alírio E. Rodrigues [a], José A.C. Silva [b,*]

[a] Laboratory of Separation and Reaction Engineering (LSRE), Associate Laboratory LSRE/LCM, Department of Chemical Engineering, Faculty of Engineering, University of Porto, Rua Dr. Roberto Frias, S/N, 4099-002 Porto, Portugal
[b] Centro de Investigação de Montanha (CIMO), Instituto Politécnico de Bragança, Campus de Santa Apolónia, 5300-253 Bragança, Portugal

A R T I C L E I N F O

Keywords:
Gas Adsorption Equilibria
Volumetric Technique
Kinetics of Sorption
Statistical Analysis
CO_2 adsorption
Binder-free 4A zeolite

A B S T R A C T

The screening of adsorbents (zeolites, MOFs, ACs, etc) requires the measurement of adsorption equilibria and kinetics at the milligram scale. In this regard, a volumetric apparatus (constant volume variable pressure – batch adsorber) has been developed for studying adsorption equilibria and kinetics of sorption. Its validation was accomplished by studying the adsorption equilibria of carbon dioxide (CO_2), methane (CH_4) and nitrogen (N_2) and the kinetics of sorption of CO_2 on commercial binder-free 4A zeolite. The data collected has an acceptable agreement with already published values by a gravimetric and breakthrough flow technique. The isotherms were modeled using Sips model from low pressure till 8 bar at 303, 343 and 373 K. The sorption kinetics of CO_2 was measured from the uptake rate experiments and fitted with a solid-film linear-driving-force model (LDF). It was observed that the LDF mass transfer coefficients increase with pressure and temperature. Finally, the statistical analysis of the data was performed by Response Surface Methodology (RSM) to determine the interactions among process variables such as temperature and pressure in the respective gas adsorption equilibria data.

1. Introduction

Nowadays, one of the world challenging issues is the global climate change and rising level of greenhouse gases (GHGs) in the atmosphere, originating from anthropogenic activities [1,2]. This environmental concern deriving from the combustion of coal, petroleum and petrochemical industries [3,4] is expected to be intensified as consequence of economic growth and industrial development [5–7]. In this context, carbon capture and storage technology has been introduced as a promising policy to reduce the GHGs emissions as well as decrease the mitigation costs of relevant industries [8]. On the other hand, due to the limitations of fossil fuels resources, attempts have been intensified to develop renewable sources of energy such as biogas [7,8]. To this end, numerous researches are devoted to find out highly efficient processes for trapping and separation of GHGs. Among different considered technologies [1], adsorption onto porous solids was introduced as one of the attractive strategies [9]. In this way, gravimetric and volumetric techniques were introduced as main techniques, which have been mainly employed for gas storage and separation studies. In the gravimetric technique, as a clear and direct method, the loading capacity is calculated by measuring the mass of sample with a magnetic suspension balance before and after experimental tests [10]. In spite of it's accuracy, this method has some drawbacks including: considering the buoyancy effect on the volume of system, lack of flexibility for multicomponent studies and high cost of the unit [11]. In return, in the volumetric technique, the uptake capacity of samples is simply calculated using the pressure drop. Checchetto et al. [10] reported that the accuracy of volumetric technique is higher than the gravimetric one since recording pressure changes is easier than measuring minor variations in the mass of sample.

The Development of the volumetric technique for measuring gas adsorption equilibria is date back to the early of 20th century, by Sieverts, which considered a glass volumetric apparatus for absorption and diffusion of gases [11]. This early volumetric apparatus passed it's evolution and was improved by pressure measurement, temperature control and performance elevation for different gas adsorption processes [12,13]. Conventional volumetric units are generally required gram-scale quantities of adsorbents [14,15], which by considering the required time to synthesis, cost and loading capacity of novel samples

---

* Corresponding authors.
E-mail addresses: mohsen.karimi@fe.up.pt (M. Karimi), jsilva@ipb.pt (J.A.C. Silva).

https://doi.org/10.1016/j.cej.2021.130538
Received 14 March 2021; Received in revised form 11 May 2021; Accepted 23 May 2021

Nomenclature

B_s	affinity constant (Sips model), -
C_b	bulk concentration, mol. cm $^{-3}$
C_{bo}	initial bulk concentration, mol. cm $^{-3}$
D	diffusivity, cm^2.s^{-1}, defined in Table 2
K	secant of adsorption equilibrium isotherm (or local slope) in respective differential sorption uptake, -
$K^{'}$	ratio between amount of sorbate in solid phase at equilibrium relatively to amount in gas phase in the respective sorption uptake, -
K_1	parameters in the temperature-dependent Sips model, mol kg $^{-1}$
K_2	parameters in the temperature-dependent Sips model, mol kg $^{-1}$ K $^{-1}$
K_3	parameters in the temperature-dependent Sips model, k Pa $^{-1}$
K_4	parameters in the temperature-dependent Sips model, K
K_5	parameters in the temperature-dependent Sips model, -
K_6	parameters in the temperature-dependent Sips model, K
k_{LDF}	linear-driving force mass transfer coefficient, s^{-1}
M	molecular weight g. mol^{-1}
m	mass of adsorbent in adsorption cell, g
n	Sips isotherm model parameter, -
P	pressure, bar
Q	adsorbed concentration, mol. kg $^{-1}$
$q_{m,s}$	saturatin adsorbed capacity, mol. kg $^{-1}$
R	universal gas constant, J mol $^{-1}$ K $^{-1}$
T	time, s
T	temperature, K
V	Volume, cm^3
$\bar{y}$	average of experimental values in RSM model
y_i	experimental values in RSM model
$\hat{y}_i$	estimated data in RSM model
Z	compressibility factor, -

Subscripts/Superscripts

A_cell	Adsorption cell
exp	experimental
cal	calculated
ref	reference cell
sor	sorbate
*	before gas expansion
n-1	previous experiment

Greek letters

ε	particle voidage
$\Re_p$	radius, cm
ρ_g	gas density, kg. m^{-3}
ρ_p	particle density, kg. m^{-3}
ε	residual error, -
ΔH_{iso}	isosteric heat of adsorption, kJ. mol $^{-1}$

(particularly in the cases of MOFs and COFs) is one of the main drawbacks of developed apparatus. On the other hand, available commercial instruments to measure isotherms volumetrically in the milligram scale have also some restrictions [16]. Generally, these type of units dońt have too much flexibility regarding studies in different adsorption systems including: 1) pressure and temperature ranges (e.g. for cryogenic studies), 2) type of adsorbents (powder, beads, pellets, 3D printed carbons, monoliths, etc.), 3) the size and the ratio of adsorption cell to the reference cell. At the same time, supplying commercial units require a high budget than home-made ones.

In the volumetric unit, the critical overview is the description of the setting up of the process and specifying the accurate volumes, including: reference volume, adsorption volume and dead volume, to acquire precise gas adsorption results [17–19]. Nevertheless, few studies have been devoted to accurate description of designing procedure and volumetric calibration as main aspects of assessment of adsorbents screening and isotherms evaluation [18–20]. In some cases, researchers [19,20] utilized the liquid technique (toluene or water) for calibrating the reference cell. This technique encompasses some problems such as using liquid to fill the reference cell is not appropriate and precise; also, this technique is offline method, which limits the capacity of this method [17]. On the other hand, detailed analyses of developed volumetric units and the calculation procedure of the absolute mass of adsorbed gases onto the adsorbents were not also well documented in the literature, while they are key elements to acquire reproductive data [21–23].

In this study, based on scope of CCS technology, a volumetric apparatus was designed, constructed and calibrated to assess the gas adsorption equilibria measurements in the milligram scale from low pressure till high pressure in a broad temperature range, with the particularity of using a circulating gas in a closed loop, to extend the measurement of data for multicomponent systems. In this way, the basic principles related with its construction, calibration procedure and data acquiring are highlighted. The unit has been developed and validated by measuring adsorption equilibria isotherms of carbon dioxide (CO_2), methane (CH_4) and nitrogen (N_2) on 4A binder-free zeolite, while other gases including hydrogen (H_2) or different adsorbents such as metal organic frameworks (MOFs), activated carbons (ACs) and etc. can also be considered in future works. Finally, uptake rate measurements were also recorded and a solid-film linear-driving-force batch adsorber model developed to calculate mass transfer coefficients related with the kinetics of sorption, and the statistical analysis of the adsorption equilibria data performed by Response Surface Methodology (RSM) strategy.

2. Experimental apparatus

2.1. Materials

In this study, the employed gases including CO_2, CH_4 and N_2 as sorbate and helium (He) as inert gas, were supplied by Air Liquide, in the following purities: CO_2 (99.98%), CH_4 (99.95%), nitrogen (N_2) (99,99%) and He (99.95%). In addition, the binder-free beads of 4A zeolite were supplied by Chemiewerk Bas Kostritz GmbH (Germany) having a diameter range of 1.6 to 2.5 mm, made from crystals of 4A zeolite with an average size around 1 μm. The synthesis and characterization of this adsorbent can be found elsewhere [24,25]. It is worth noting this adsorbent has been studied in this work because of the following reasons: first of all, 4A zeolite has a higher selectivity for separating mixtures of CO_2/N_2 and $CO_2/CH_4/N_2$ than other competitive zeolites (e.g., 13X zeolite), which nominates it as an excellent candidate for separation processes on post-combustion and biogas upgrading adsorption technologies [26–28]. Also, the small pore size of zeolite 4A allows the measurement of reliable kinetic mass transfer coefficients for CO_2 in macroscopic systems (if uptake rate data is properly analyzed) [24]. Furthermore, the adsorbent studied is relatively in a new form of binder-free beads that is available for large-scale applications [29].

2.2. Equipment design

The volumetric apparatus contains two independent volumes including a reference cell and adsorption cell, which are connected by a needle valve. The pressure variations are monitored/recorded by a pressure transducer with high accuracy of ± 0.08% BSL (linearity, hysteresis and repeatability combined) and long-term stability (1-Year), ±0.1% full scale (FS) typical, in a pressure range of 0–50 bar (provided by Omega Co.). The considered cells were designed in a batch loop, which circulates the adsorbate gases by a circulating pump, operating in the pressure range of −100 mbar (vacuum) till 150 bar. (Thomas Co.). This arrangement is important for extending the unit to multicomponent adsorption equilibria studies [13,14]. The temperature of the reference cell volume and adsorption cell are controlled by a thermocouple and a chromatographic oven, respectively. The temperature of the chromatographic oven covers the maximum temperature of 623 K (SRI Co). Also, the helium flow rate during the desorption step (for the regeneration of the adsorbent) was controlled via a mass flow controller (MFC), with operation rate of 0 to 100 ml/min and an accuracy of ± 1.0% full scale (Aalborg Co.). In addition, a vessel with a volume of 40 cm^3 was employed for calibration of the total volume of the system. All other tubing, fitting and adaptors were 316 stainless steel in 1/8″ diameters, supplied by Swagelok Co. All detailed description of this apparatus is reported in Table S1 (Supporting Information).

2.3. Volumes calibration

The designed volumetric apparatus is depicted in Fig. 1. Knowing accurately the volumes of the reference and adsorption cells and all dead volumes are fundamental steps for the adsorption equilibria studies. To this end, a vessel by 40 cm^3 volume was employed for the calibration procedure. Initially, all parts of the unit remain under vacuum, then a certain pressure of helium gas (15 bar) was fed to the calibration vessel, after that, valve-6 was closed and the system depressurized to the atmospheric pressure. Now, the residual volume, which is the line between the vessel and other cells (specified by light blue in Fig. 1), was determined by opening the valve-6, while other valves (V-5, V-7, V-9, V-14) were closed. This volume was calculated by recording the new pressure and employing the ideal gas law (PV = nRT). Then, once again, by closing the V-6, the unit was depressurized to the atmospheric pressure. In a similar procedure, by knowing the gas pressure in the vessel (from the previous step), the volume of reference cell was calculated. At the end, while the residual volume and reference cell have already been specified, by pressurizing the calibration vessel to 15 bar, the volume of adsorption cell was determined. Specific properties and calibration details of the developed unit are presented in Table 1.

Table 1
Specific properties and calibration details of the developed volumetric unit.

Specific Properties of 4A Binder-less Zeolite (4A BFK 1.6–2.5 mm) [24]		
Parameter	Numerical Values	unit
Total Intrusion Volume	3.5×10^{-4}	$m^3\ kg^{-1}$
Surface Area (Mercury intrusion)	3.49×10^3	$m^2\ kg^{-1}$
Surface Area (CO_2 Physisorption)	5.01×10^5	$m^2\ kg^{-1}$
Average Pore Diameter	3.61×10^{-7}	m
Apparent Density	1109	$kg\ m^{-3}$
Solid Density	1707	$kg\ m^{-3}$
Skeleton Density	2225	$kg\ m^{-3}$
Volumes of Specific Parts of the Unit		
Parameter	**Numerical Value**	**unit**
Reference Volume	44	cm^3
Adsorption Cell	2.5	cm^3
Residual Volume	0.8	cm^3
Mass of Adsorbent Used in the Experiments and Ambient Air Conditions		
Parameters	**Numerical Value**	**unit**
Mass of Raw Sample	~0.437	g
Mass of Activated Sample	~0.402	g
Ambient Temperature	298	K
Ambient Pressure	1	bar

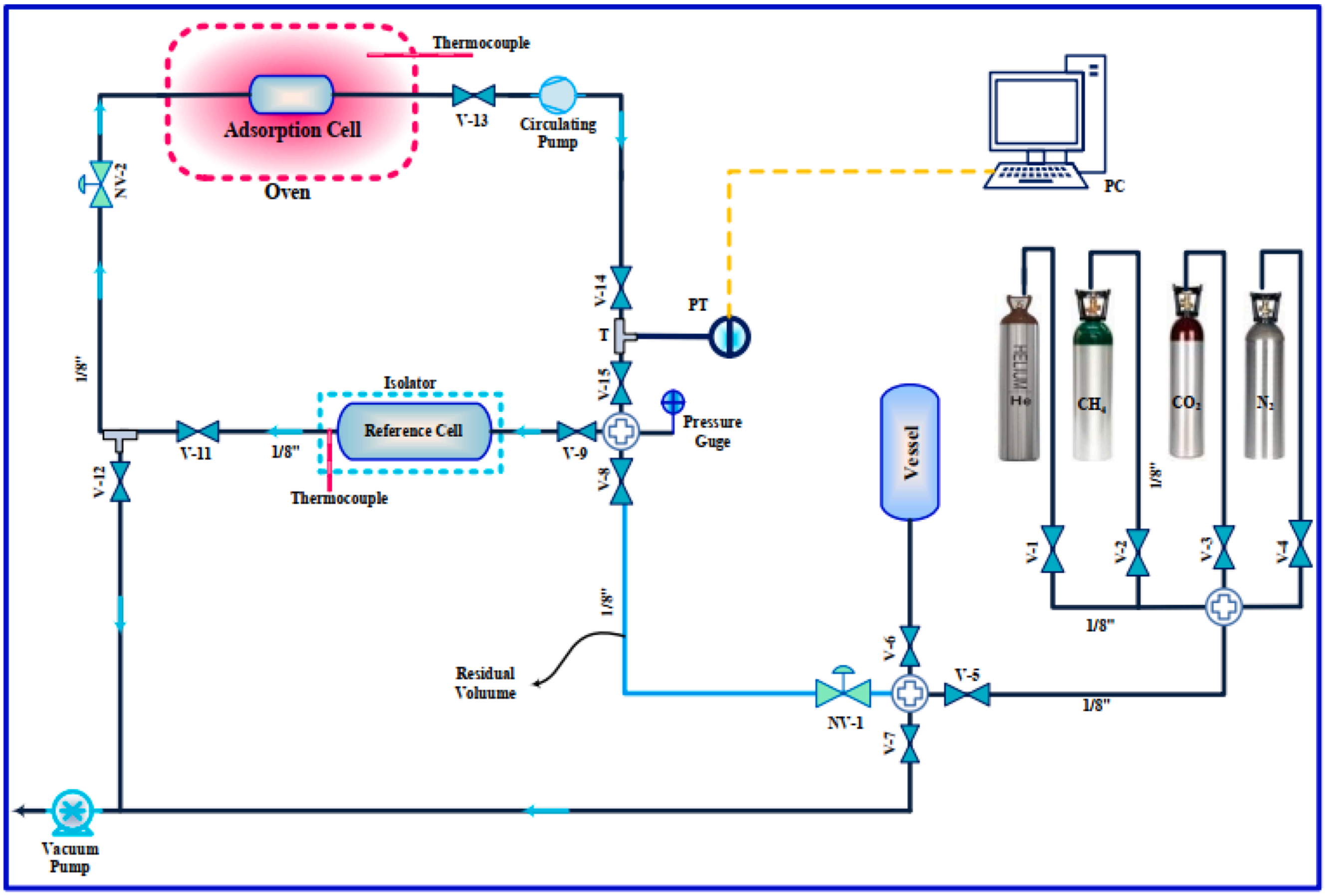

Fig. 1. Detailed description of the developed volumetric unit for measuring gas adsorption equilibria and kinetics of sorption.

3. Operation of the volumetric apparatus

3.1. Experimental procedure

Prior to data acquisition and measurement of the adsorption equilibrium isotherms, the following steps were required. First the adsorption cell was charged by the adsorbent sample, then to remove any moisture or impurities, the sample was activated by passing the helium gas in the adsorption cell (with a flowrate of 20 ml/min) at 573 K, under vacuum, by a heating rate of 1 K/min and let thereafter at a constant during a period of at least 12 h. During the activation process, valves (V-7 and V-11) were closed and other valves opened. The experimental methodology of the volumetric technique (constant volume variable pressure) consists of sequential steps of gas injection to the adsorption cell (pressure steps), following the subsequent change of pressure due to the change of the amount adsorbed in the approach to a new equilibria state under the desired operating conditions. For starting the gas adsorption measurements, pure gas (CO_2, CH_4 or N_2) was introduced to the reference cell, while valves (V-7, V-11: V-14) were closed to supply the reference pressure. Then, V-8 was closed and V-11 and NV-2 were opened, afterwards, the adsorption process started. Following this, V-13 & V-14 were opened and the circulating pump was turned on, simultaneously. The pressure was continuously monitored and recorded until the new equilibrium condition is attained. This procedure was repeated as many times as the number of steps needed (by considering small pressure steps) to set-up the adsorption equilibrium isotherm. It is worth mentioning that before all pressure steps, including: calibration, activation and experimental tests, the leak test was performed by expanding the inert gas (Helium) to the system at high pressure (around 20 bar) and ambient temperature (for at least 12 h).

3.2. Data treatment

The volumetric principle is a straightforward technique for gas adsorption measurement [30,31]. Each run contains two fundamental steps including: gas injection to the reference cell and gas expansion to the adsorption cell. The amount of sorbate gas on the adsorbent is simply calculated by measuring the pressure variations between the initial and final equilibrium uptake. In this way, a mass balance is applied on the control volume. Hence, the mass of sorbate in the system, before expanding the gas to the adsorption cell (when valves V-11 and NV-2 are closed in Fig. 1), is calculated by [19,20]:

$$m_1 = m^*_{ref} + m^*_{A\_cell,n-1} + m_{sor,n-1} \tag{1}$$

here, m^*_{ref} is the mass of gas in the reference cell, also $m^*_{A\_cell,n-1}$ and $m_{sor,n-1}$ indicate the mass of gas in the adsorption cell and the sorbate amount from the previous step. Next, the mass of sorbate after gas expansion is measured by:

$$m_2 = m_{ref} + m_{A\_cell} + m_{sor} \tag{2}$$

which, m_{ref}, m_{A-cell} and m_{sor} are the same variables from the previous step for new adsorption equilibrium condition. Now, by employing the law of conservation of mass and considering: '$mRTZ = PVM$', one can measure the amount of sorbed gas by [19,20]:

$$m_{sor} = \frac{M}{RZT}\left[P^*_{ref}V_{ref} + P^*_{A\_cell,n-1}V_{A\_cell} - P_{ref}V_{ref} - P_{A\_cell}V_{A\_cell}\right] + m_{sor,n-1} \tag{3}$$

here, M is the molecular weight of gas, R and Z are the universal gas constant and compressibility factor, respectively. Also, P, T and V indicate the pressure, temperature and volumes of reference and adsorption cells before and after gas expansion (more details can be found in Nomenclature). This equation simply shows that the loss of mass in the control volume is balanced by obtaining the mass sorbed by adsorbent particles. Then, the adsorbed amount ($q'(mol/kg)$) is calculated by considering the molar weigh of sorbate gas and mass of sample. Afterwards, to obtain the absolute adsorption value, based on the Gibbsian surface model, a correction is required [32–35], which is expressed by:

$$q = q' + \nu_P \rho_g \tag{4}$$

that ν_P and ρ_g are the specific pore volume of the adsorbent and the gas density at the equilibrium temperature and pressure, respectively [35,36].

4. Theory

4.1. Adsorption equilibrium

In the recent decades, several isotherm models have been proposed for the description of the adsorption equilibria [37]. All of the proposed models are dominated by three major principles including: kinetic considerations, thermodynamics and potential theory [37–40]. Among the different adsorption equilibrium isotherm models, Langmuir, dual-site-Langmuir, Freundlich and Sips can be considered for describing Type I isotherms, that is the most frequent type observed in commercial zeolites [41]. The empirical Sips isotherm as a combination of both Langmuir and Freundlich models is very flexible for modelling gas adsorption equilibria for the design of adsorption processes, which is defined by:

$$q = \frac{q_{m,s}(B_sP)^{1/n}}{1 + (B_sP)^{1/n}} \tag{5}$$

here $q_{m,s}$ and B_s are the saturation capacity and affinity constant, respectively and n is a parameter that describes the degree of heterogeneity of the adsorbent that is generally higher than unit. To obtain an acurate description of the equilibrium data in different temperature ranges, it is helpful to develop an isoherm model considering the temperature dependency for its parmeters [42]. In this sense, the saturation capacity parameter of the Sips model$\left(q_{m,s}\right)$ can be calculated by:

$$q_{m,S} = K_1 + K_2T \tag{6}$$

Also, the affinity constant (B_S) and exponent (n) based on the temperature-dependent Sips isotherm model are defined by [42–44]:

$$B_S = K_3exp(K_4/T) \tag{7}$$

$$n = K_5 + K_6/T \tag{8}$$

In this study, the standard deviation between model values and experimental data is calculated by:

$$S_D = \sqrt{\frac{1}{N}\sum_{i=1}^{N}\left(q_i^{exp} - q_i^{cal}\right)^2} \tag{9}$$

4.2. Isosteric heat of adsorption

In this study, the isosteric heat of adsorption was also estimated using the Clausius-Clapeyron equation as [44,45]:

$$(-\Delta H_{iso}) = RT^2\left(\frac{\partial lnp}{\partial T}\right)_{q=constant} \tag{10}$$

where P, $T$and R are the gas pressure, the temperature of system and universal gas constant, respectively. Also, $\Delta H_{iso}$is the isosteric heat of adsorption, assuming its independency from temperature, and by integrating from Eq.10, one can obtain [46–48]:

$$lnp = constant - \frac{\Delta H_{iso}}{RT} \tag{11}$$

Eq. (11) is a useful tool to calculate the isosteric heats of adsorption directly from the experimental data.

4.3. Kinetics of sorption

A solid-film-resistance linear-driving-force model (L.D.F) was considered to describe the mass transfer of the sorbate between the bulk gas and solid phases in the volumetric unit studies, which provides a mathematically simple description for the sorption kinetics, from where the rate coefficients are a valuable tool to describe the dynamics of sorption in fixed bed columns [49].

This approach developed by Sircar [50] for describing the kinetics of experimental uptake rate data for constant sorbate concentration surrounding the adsorbent (infinite system), is applied now here to obtain the kinetic information from the transient uptake in the case of constant volume variable pressure batch adsorber (finite system), also called piezometric system. Do and Rice [51] developed a solution that can applied for this case by assuming a parabolic profile of the sorbate inside the adsorbent particles (similar as the LDF approach). The solution is presented here (with an appropriately redefinition of the variables) for the direct calculation of the mass-transfer coefficient k_{LDF}, based on the Glueckauf approximation for a spherical particle (where k_{LDF} is equal to $15D/R^2$), being the solution for the uptake rate for an isothermal system (finite system volume variable pressure) of the batch adsorber given by:

$$\frac{C_b}{C_{b0}} = \frac{1}{(K'+1)} + \frac{K'}{(K'+1)} exp[-(1+K')k_{LDF}t] \tag{12}$$

where Cb andC_{bo} are the bulk and initial bulk gas concentration (pressure), respectively, K' is the ratio between the amount of sorbate in the solid phase at the equilibrium relatively to the amount in the gas phase in the respective sorption uptake given by $K' = \frac{(m/\rho_p)K}{V}$. Also, K is the secant of the adsorption equilibrium isotherm taken between the initial and final pressure uptake or the respective differential slope assuming it as being practically linear in such range, as well as k_{LDF} is the so-called linear-driving force mass transfer coefficient. If we define now the fraction of the sorbate adsorbed by the adsorbent as $\lambda \equiv \frac{C_{b0}-C_{b\infty}}{C_{b0}}$, where $C_{b\infty}$ is the final equilibrium concentration and take $K' = \frac{\lambda}{1-\lambda}$, we can get the fractional uptake curve for the batch adsorber for a finite system volume as,

$$F(t) = \frac{C_{b0} - C_b}{C_{b0} - C_\infty} = 1 - exp[-(1+K')k_{LDF}t] \tag{13}$$

For very small values of K' (infinite media) the result for an isothermal system is the one shown by Sircar [50]:

$$F(t) = \frac{C_{b0} - C_b}{C_{b0} - C_\infty} = 1 - exp[-k_{LDF}t] \tag{14}$$

It is evident that by comparing the fractional uptake calculated from Eqs (13) or (14), the effect of constant volume variable pressure appearing in (Eq (13)) (through parameter K') will lead to the calculation of a erroneously high apparent value for k_{LDF} if neglected (Eq. (14)), a result already highlighted by Ruthven [45].

Eqs (12) or (13) for the constant volume variable pressure system have two parameters: $\acute{K}$ and k_{LDF}, which one of them can be estimated from the respective sorption uptake ($\acute{K}$), and the other one (k_{LDF}) calculated by the best fit of the experimental uptake rate data by minimizing the error between the experimental and calculated values (Eq. 12 or 13). The previous equations can be a valuable tool for a rough estimation of the lumped k_{LDF} mass transfer coefficient, useful for the dynamic simulation and design of fixed bed adsorption processes [49], calculated from independent piezometric studies in volumetric adsorption equilibria measurement units.

4.4. Statistical analysis by RSM

Response surface methodology (RSM) as a combination of statistical and mathematical methods is a robust computing approach to experiments design, statistical analysis, optimization, and detecting the interaction effects [52,53]. The first step to develop a RSM model is finding the main independent variables of process as factors of the model, which are defined in three levels coded as -1, 0 and $+1$ [54,55]. Then, various regression analyses are employed to determine the interaction effects between the considered factors and develop surface response [56]. In this study, the statistical analysis of equilibrium adsorption data was accomplished by considering the equilibrium pressure (Pe) and adsorption temperature as main factors (independent variables), which determine the adsorption loading (q) as response of the process. In this sense, the analysis of the obtained experimental values as well as the interaction effects of parameters have been evaluated using the Historical Data tool of the Design Experts software v.8.0 [1,57]. Afterwards, a quadratic polynomial function was employed for fitting the experimental values, which contributes to:

$$y = \beta_0 + \beta_1 x_1 + \beta_2 x_2 + \beta_{12} x_1 x_2 + \beta_{11} x_1^2 + \beta_{22} x_2^2 + \varepsilon \tag{15}$$

Here, x_1 and x_2 represent the independent variables, and y is the response surface. $\beta_1$and $\beta_2$are the linear coefficients of independent variables, while the interaction effect between the main factors is expressed by β_{12}. Also, $\beta_{11}$and β_{22} are the quadratic coefficients of operating conditions. In addition, β_0 and ε indicate the intercept coefficient and residual error, respectively [1,57]. Then, the statistical evaluation of developed model was performed to determine the best coefficients of the quadratic model for experimental values as a significant model by using the analysis of variance (ANOVA) [55]. It is worth mentioning that a significant model should have a non-significant lack-of-fit and acceptable p-values [1,55]. Finally, the accuracy of model is determined by evaluating the regression coefficients (R^2 and adjusted R^2) and the standard deviation, which defined by [56,57]:

$$R^2 = 1 - \frac{\sum_{i=1}^{n}(y_i - \hat{y}_i)^2}{\sum_{i=1}^{n}(y_i - \bar{y})^2} \tag{16}$$

$$AdjR^2 = 1 - \frac{(1-R^2)\cdot(n-1)}{(n-P-1)} \tag{17}$$

$$Std.Dev. = \sqrt{\frac{\sum_{i=1}^{n}(y_i - \hat{y}_i)^2}{n-P}} \tag{18}$$

here, y_i, $\hat{y}_i$, and $\bar{y}$ represent the experimental results, estimated data, and the average of experimental values, respectively. Also, P and n are the numbers of predictors and experiments, respectively [52,57].

5. Results and discussion

The adsorption equilibria data of CO_2, CH_4 and N_2 on binder-free 4A zeolite by the developed volumetric apparatus in this work were compared with the one measured from gravimetry in a magnetic suspension microbalance, which has recently been studied [24]. There is also a promising similarity with the one obtained by a breakthrough technique [58]. Moreover, each compound has a different behavior on binder-free 4A zeolite with a significantly different loading capacity, which is also important to validate the performance of the unit in different kind of sorbate-sorbent adsorption equilibria interactions.

5.1. Adsorption equilibrium isotherms

The adsorption equilibrium isotherms of CO_2, CH_4 and N_2 at 303, 343 and 373 K obtained by the developed volumetric unit are represented in Figs. 2-4, respectively. As previously discussed, the Sips model isotherm was applied to describe the experimental adsorption equilibrium data of CO_2, CH_4 and N_2 on binder-free 4A zeolite, where the parameters are shown in Table 2. As expected, the hierarchy order of the adsorption amount is $CO_2 \gg CH_4 > N_2$, being the adsorption capacity of

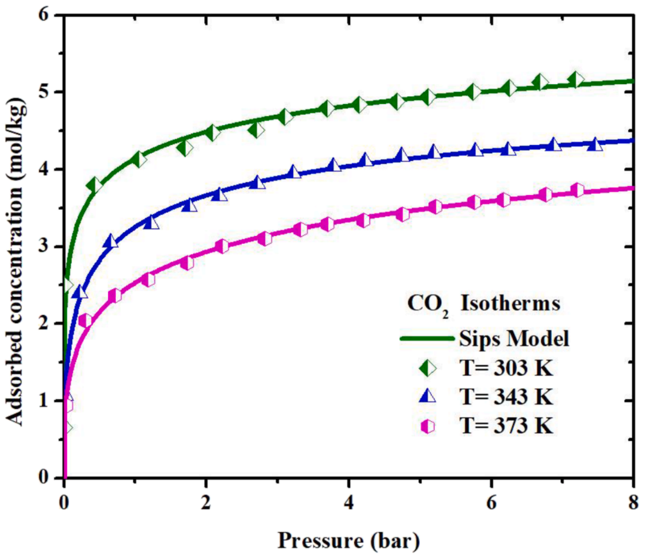

Fig. 2. Adsorption equilibrium isotherms of CO_2 on binder-free 4A zeolite at 303, 343 and 373 K measured in the volumetric unit and fitting with the Sips model.

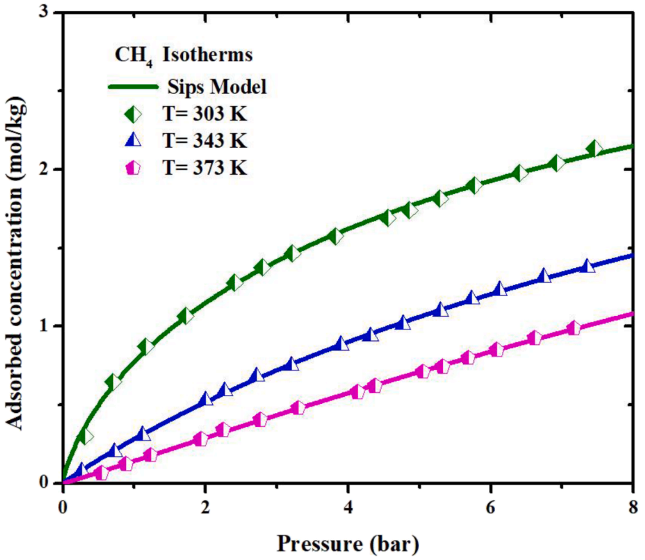

Fig. 3. Adsorption equilibrium isotherms of CH_4 on binder-free 4A zeolite at 303, 343 and 373 K measured in the volumetric unit and fitting with the Sips model.

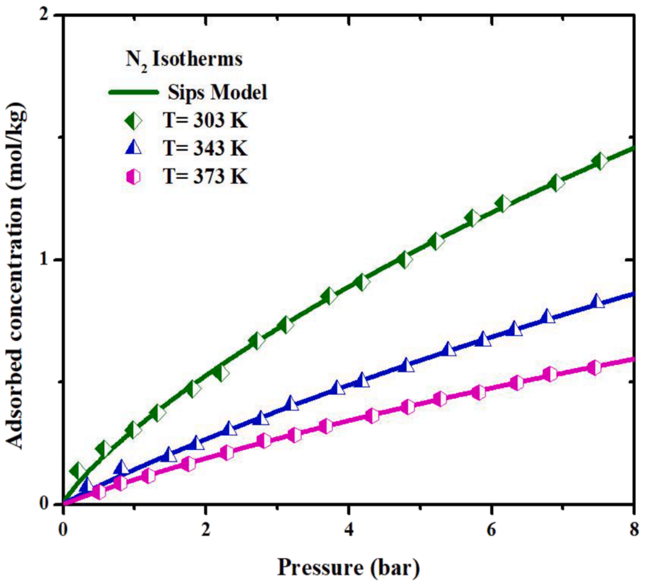

Fig. 4. Adsorption equilibrium isotherms of N_2 on binder-free 4A zeolite at 303, 343 and 373 K measured in the volumetric unit and fitting with the Sips model.

CO_2 significantly higher at the lower pressure than for the other sorbates. The isotherms measured in this work and the ones reported by using a gravimetric apparatus (the same samples) [24], are compared in the Supporting Information (Appendix B). In addition, a comparison between adsorption equilibria values of 4A zeolite for CO_2, CH_4 and N_2 loading using different adsorption techniques is also provided in the Supporting Information (Appendix C). As can be seen in Figs. S1-S-3, there is a close agreement between the values obtained by both methods, which validates the performance of designed volumetric unit for measuring gas adsorption equilibria. **Isosteric Heat of Adsorption**

The isosteric heat of adsorption for the CO_2, CH_4 and N_2 calculated by the Clausius–Claypeyron equation (Eq. (10)) is shown in Fig. 5. As can be seen, the heat of adsorption follows the order $CO_2 > CH_4 > N_2$, also it has a decreasing pattern by increasing the loading. It is worth noting that the isosteric heat of adsorption of zeolite 4A for CO_2, CH_4 and N_2 were already reported in the literature around 40, 20 and 15 $kJ.mol^{-1}$, respectively [24,47,48], which are in the same range of the observed values in this study.

5.2. *Kinetics of sorption*

The estimation of intrinsic mass transfer coefficients for the kinetics of sorption taken from uptake rate data measured in constant volume variable pressure (piezometric system) its not an easy task, due to the possible intrusion of several extraneous effects in the respective kinetic uptake especially in fast systems such as: 1) heat effects due to sorption inside the column and respective dynamics of heat transfer to the surroundings; 2) time constants from manifold valve opening; 3) integral of differential diffusivities dependent of pressure step size; 4) extraneous diffusion in the bed of porous particles, etc [45]. And most important of all as shown by Barrer [59], since the volumetric system is itself a macroscopic system the determination of time constants of diffusion will be restricted to the half time of the uptake curve $t_{1/2}$, which is simply for a micropore diffusion control system equal to $2.x10^{-2}\ r_c^2/D_c$ (r_c is the radius of crystallites and D_c the micropore diffusivity) or for a macropore diffusion control equal to $2.x10^{-2}\ R_p^2\ (1+K)/D_p$, ($R_p$ is the radius of beads and D_p the macopore diffusivity), which means for example that for half of the uptake and a particle with a crystal size of around 1 μm (the size of most of the available commercial pellets/beads of zeolite materials) the only allowable diffusivity to be calculated in a half time response of 2.1 s in a volumetric/piezometric system is below $1x10^{-14}$ m^2/s .

Taken into account all these previous described limitations, an estimate of the sorption kinetics of CO_2 calculated from selected uptake rates during the measurement of the adsorption equilibria data shown in section 5.1 is possible (without too much error), being reported here using the simplified kinetic model described previously in section 4.3. For CH_4 and N_2 such data is impossible to measure since the uptake rates were too fast and data is unreliable. In this way, the calculation of the lumped mass transfer coefficients (k_{LDF}) from selected uptake rates of CO_2 (where most of the previous described extraneous effects are minimal) was performed using the batch adsorber model by applying Eq. (12), and minimizing the error between the experimental and calculated values. For such purpose, only some experimental uptake rates were chosen (taken from small pressure steps) especially at the higher loadings, where the slope of the isotherm is relatively small (between the

Table 2

Adsorption isotherm parameters of Sips model (temperature-dependent model) for CO_2, CH_4 and N_2 onto binder-free 4A zeolite.

Sips Model Isotherm Parameters				Temperature-dependent parameters		S_D		
Gas:	T (K)	$q_{m,s}(mol/kg)$	B_S	n	K_1	$K_2 \times 10^3$	K_3	
					K_4	K_5	K_6	
CO_2	303	7.52	2.11	3.65	7.38	0.411	2.11	0.08
					0.003	3.57	24.27	
	343	5.68	1.94	2.27	5.54	0.403	1.94	0.04
					0.003	2.23	16.04	
	373	5.12	0.27	1.76	3.09	0.392	0.26	0.05
					0.003	1.59	14.52	
CH_4	303	4.16	0.136	1.35	0.003	0.887	14.639	0.02
						1.294	15.864	
	343	4.10	0.067	1.036	3.976	0.398	0.067	0.01
					0.003	0.989	14.846	
	373	4.08	0.033	0.934	5.357	0.403	0.033	0.006
					0.003	0.887	14.639	
N_2	303	3.28	0.017	1.222	5.162	0.4	1.233	0.02
					0.003	0.506	13.950	
	343	3.12	0.020	1.070	5.338	0.403	0.02	0.01
					0.003	1.022	14.910	
	373	2.99	0.028	1.063	2.848	0.455	0.028	0.004
					0.002	1.011	16.376	

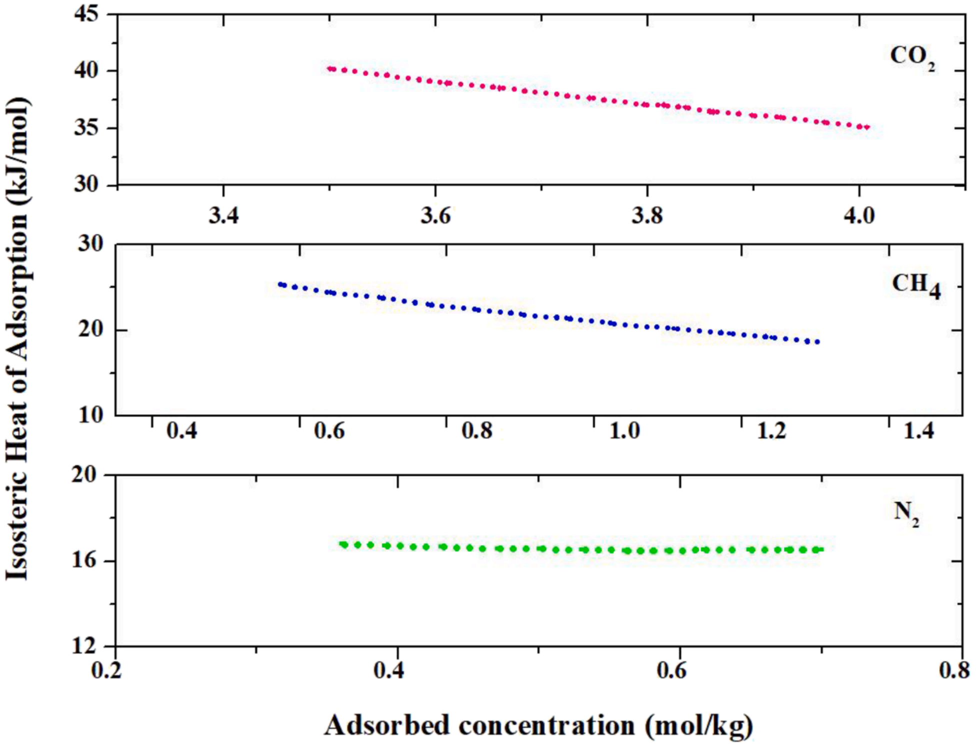

Fig. 5. Isosteric heats of adsorption on binder-free 4A zeolite for CO_2, CH_4 and N_2 as a function of the adsorbed amount in the temperature range of 303–373 K.

initial and final equilibrium conditions), being in this way at the same time, the amount adsorbed in the uptake also small to decrease the intrusion of possible heat effects. Fig. 6 shows the selected uptake rate experiments and the respective fitting values. Also, the calculated parameters of the mass transfer coefficient (k_{LDF}) are reported in Table 3. As shown in Fig. 6, there is an acceptable agreement between experimental and modeling results. Furthermore, as can be seen in Table 3, at all considered temperatures, as the pressure and loading increase the uptake rates become faster. The k_{LDF} values range from 0.029 to 0.128 s^{-1} between pressures 0.15 and 1.04 bar at 303 K. The same behavior is observed at the higher temperatures, where the value of k_{LDF} can reach 0.467 s^{-1} at the pressure of 1.18 bar at 373 K. Several explanations can be drawn for this pressure dependent behavior of the k_{LDF} parameters such as the decreasing slope of the isotherm as the pressure increases (assuming the system is dominated by a macropore diffusion control) [45], or the respective thermodynamic correction factor due to the increasing loading according to the Darken relation (considering the system is dominated by a micropore diffusion control) [59], or a mix of both effects lumped in the k_{LDF} parameter calculated. It is clear from Fig. 6 that the enhancement of pressure and temperature lead to fast uptake rates. In addition, the average values of the activation energy for the k_{LDF}mass transfer coefficients are in the order of 19.5 kJ/mol. It

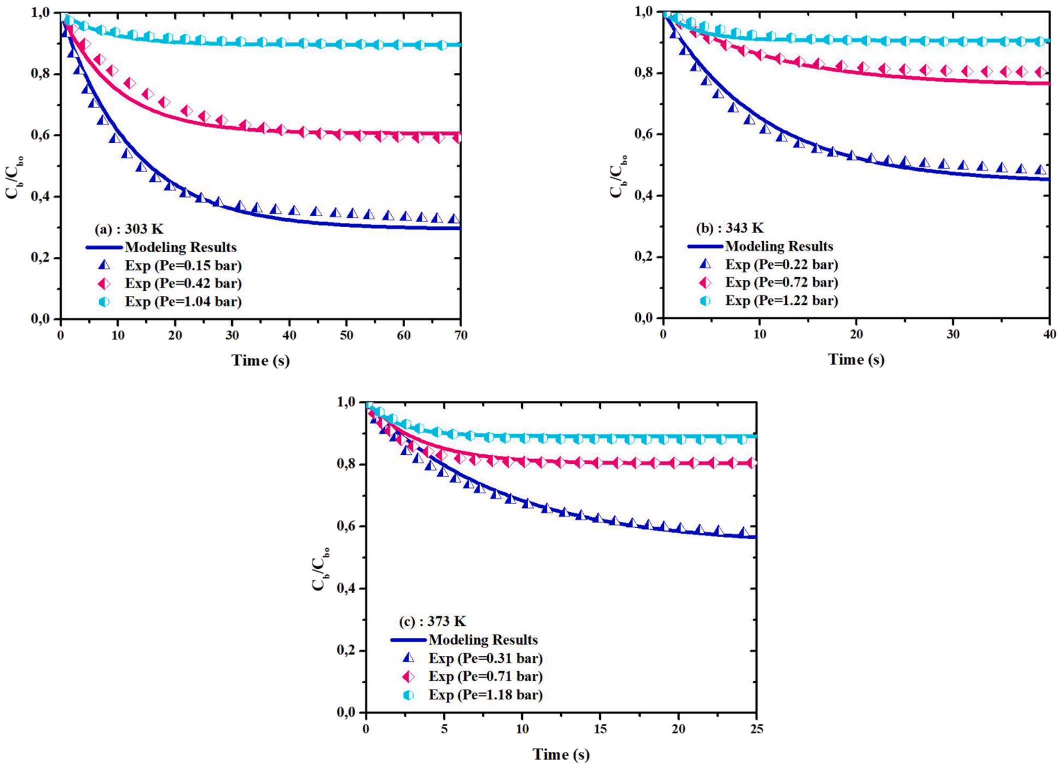

Fig. 6. Uptake rate experiments of CO_2 at selected pressures and fitting with the batch adsorber model (Eq. (12)) at: **(a)** 303 K, **(b)** 343 K and **(c)** 373 K.

Table 3
Mass transfer (k_{LDF}) parameters calculated from the fitting of the batch adsorber model (Eq. (12)) to the uptake rate data shown in Fig. 6.

	$P_e(bar)$	K'_{exp}	$K'_{mod\ el}$	$k_{LDF}(s^{-1})$*
T = 303 K				
Run-1	0.15	2.14	2.21	0.029
Run-2	0.42	0.69	0.64	0.078
Run-3	1.04	0.14	0.12	0.128
T = 343 K				
Run-1	0.22	1.12	1.24	0.049
Run-2	0.72	0.24	0.31	0.082
Run-3	1.22	0.12	0.10	0.317
T = 373 K				
Run-1	0.30	0.73	0.85	0.068
Run-2	0.71	0.24	0.25	0.287
Run-3	1.18	0.14	0.12	0.467

* Estimated activation energy: 19.5 kJ/mol.

Table 4
The results of analysis of variance (ANOVA) for the proposed polynomial models for CO_2, CH_4 and N_2 using multiple regression analysis.

CO_2	Sum of squares	Mean squares	Coded Coefficient	Standard error	df	p-Value
Model	27.95	6.99			4	<0.0001
T	15.40	15.40	−0.71	0.031	1	<0.0001
P	11.26	11.26	0.85	0.043	1	<0.0001
T × P	0.026	0.024	−0.048	0.053	1	0.3674
P^2	1.90	1.90	−0.66	0.081	1	<0.0001
Residual	1.15	0.029			40	–
Total	29.11	–			44	–
CH_4						
Model	14.23	2.85			5	< 0.0001
T	3.10	3.10	−0.32	0.011	1	< 0.0001
P	6.60	6.60	0.72	0.017	1	< 0.0001
T × P	0.28	0.28	−0.092	0.011	1	< 0.0001
T^2	0.12	0.12	0.037	6.569×10^{-3}	1	< 0.0001
P^2	0.17	0.17	−0.19	0.029	1	< 0.0001
Residual	0.15	3.856×10^{-3}			39	
Total	14.38				44	
N_2						
Model	4.55	0.91			5	< 0.0001
T	1.87	1.87	−0.25	3.293×10^{-3}	1	< 0.0001
P	2.91	2.91	0.44	4.555×10^{-3}	1	< 0.0001
T × P	0.34	0.34	−0.19	5.646×10^{-3}	1	< 0.0001
T^2	0.059	0.059	0.079	5.771×10^{-3}	1	< 0.0001
P^2	0.011	0.011	−0.051	8.631×10^{-3}	1	< 0.0001
Residual	0.012	3.152×10^{-3}			39	
Total	4.57				44	
	CO_2	**CH_4**	**N_2**			
Std. Dev.	0.17	0.062	0.018			
R^2	0.9604	0.9895	0.9973			
Adj-R^2	0.9565	0.9882	0.9970			
Pred-R^2	0.9334	0.9829	0.9961			

should be noted that the calculated values of k_{LDF}at 303 K shown in this work are in the same order of the ones reported recently by Streb and Mazzotti [49]. They reported linear driving force mass transfer coefficients for CO_2 in commercial zeolite 13X beads (a much open channel structure than zeolite 4A) around 0.06 s^{-1} at 298 K, being the values also used also to simulate the dynamics of cyclic adsorption processes (VSA) [60].

5.3. Statistical analysis

The statistical analysis of the volumetric equilibrium results was performed by the Historical Data tool of RSM. To this end, the equilibrium values, which have been reported in Supporting Information (Appendix C), were introduced as input values to develop the models. Then, the significance of models and regression analyses were accomplished by Analysis of Variance (ANOVA) to determine the lack of fits, p-values, interaction effects as well as the accuracy of models. The regression analysis for CO_2, CH_4 and N_2 uptake is provided in Table 4. Also, the response surfaces for non-coded values of independent values result in:

$$q_{CO_2} = 9.037 - 0.019T + 0.705P - 3.68 \times 10^{-4}T \times P - 0.047P^2 \tag{19}$$

$$q_{CH_4} = 13.52 - 0.072T + 0.73P - 1.29 \times 10^{-3}T \times P + 9.34 \times 10^{-5}T^2 - 0.015P^2 \tag{20}$$

$$q_{N_2} = 7.91 - 0.045T + 0.64P - 1.46 \times 10^{-3}T \times P + 6.46 \times 10^{-5}T^2 - 3.85 \times 10^{-3}P^2 \tag{21}$$

According to the ANOVA results (Table 4), developed models are significant accompanied by acceptable values for Standard Deviation, R^2, Adj-R^2 and Pred-R^2, which demonstrate the accuracy of obtained approaches. Also, coded coefficients indicate that the linear coefficients have determinative effects on the dependent variable than other ones (which include: −0.71 & +0.85 for T & P of CO_2, −0.32 & 0.72 for T & P of CH_4, and −0.25 & 0.44 for T & P of N_2). In addition, the negative values of temperature and positive amounts of pressure for linear coefficients are in accordance with the Le Chatelier's principle, which elucidates the negative and positive effects of temperature and pressure, respectively, on adsorption process [1]. Furthermore, these coefficients demonstrate that the pressure dependency is the dominate factor in all developed approaches. The ANOVA reveals that there are more interaction effects between considered factors for N_2 adsorption over CO_2 and CH_4. Regarding the surface plots (Fig. 7), as can be expected, pressure increment resulted in the increase of adsorption loading in all response surfaces, while the temperature enhancement has reduced the uptake capacity. In addition, one can find in plots of Fig. 7, that the pressure has a lower effect on equilibrium adsorption in the higher temperatures [42,44].

6. Conclusion

A simple volumetric apparatus was developed for measuring gas adsorption equilibria and kinetics of sorption with samples of adsorbent at the milligram scale, using a circulating gas with the possibility to extended studies for multicomponent gas adsorption. The unit was validated with binder-free beads of 4A zeolite for CO_2, CH_4 and N_2 adsorption from low pressure till 8 bar at 303, 343 and 373 K, by comparing the volumetric results with available gravimetric and dynamic data available in literature. The Sips isotherm model (with temperature dependent parameters) was employed to fit the CO_2, CH_4 and N_2 adsorption equilibrium data. The results showed an acceptable agreement between the adsorption equilibrium model and experimental values. The isosteric heat of adsorption was also calculated for CO_2, CH_4 and N_2 with values around 40, 20 and 15 $kJ.mol^{-1}$, respectively. In addition, the kinetics of sorption of the system was investigated from uptake rate experiments for CO_2. To this end, a developed batch adsorber kinetic model (constant volume variable pressure) was employed by considering a solid-film-resistance linear-driving-force approach (LDF) for mass transfer. The values of the respective calculated k_{LDF} parameters for CO_2 range between 0.029 and 0.128 s^{-1} at 303 K, 0.049–0.317 s^{-1} at 343 K, and 0.068–467 s^{-1} at 373 K, all pressure dependent at each temperature, but in the same range of already published data in commercial zeolite adsorbents. Furthermore, the statistical analysis of measured equilibrium values was performed by RSM strategy that proved the true behavior of developed unit and specified the interaction parameters of the adsorption process. Finally, it can be concluded that the simple designed volumetric unit is a valuable tool for measuring adsorption equilibrium data and kinetics of sorption, which by reporting all detailed descriptions and specifications of unit, as well as discussing calibration and validation procedures can be a helpful study for other adsorptive design processes.

Declaration of Competing Interest

The authors declare that they have no known competing financial interests or personal relationships that could have appeared to influence

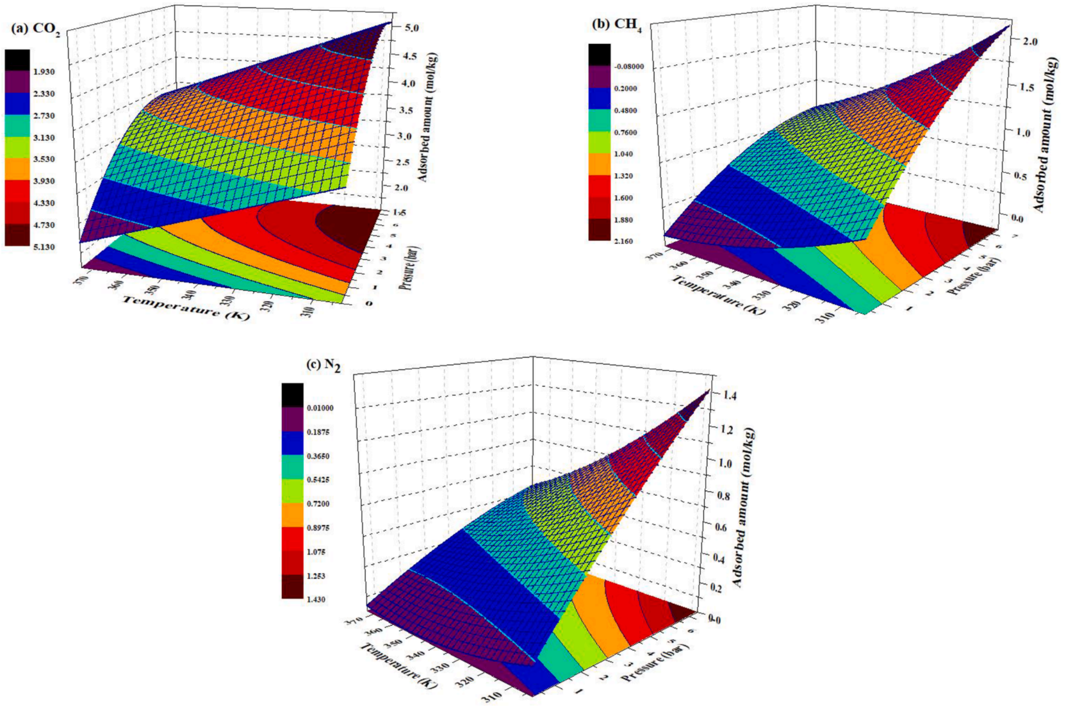

Fig. 7. Response surface plots for: **(a)** CO_2 **(b)** CH_4 and **(c)** N_2 adsorbed amount (mol/kg) as a function of equilibrium pressure (bar) and adsorption temperature (K).

the work reported in this paper.

Acknowledgments

Authors would like to acknowledge Kristin Gleichmann and Chemiewerk Bad Koestritz GmbH for kindly providing the binder-free beads of 4A zeolite. This work was financially supported by: 1) Project ″VALORCOMP″ (ref.0119_VALORCOMP_2_P), financed through INTERREG V A Spain Portugal (POCTEP) 2014-2020, under the European Regional Development Fund (ERDF). 2) Project POCI-01-0145-FEDER006984-Associate Laboratory LSRE-LCM funded by ERDF through COMPETE2020, Programa Operacional Competitividade e Internacionalização (POCI), and by national funds through Foundation for Science and Technology (FCT, Portugal) and ERDF under Programme PT2020 to CIMO (UID/AGR/00690/2019); 4) M. Karimi also recognizes a PhD research grant awarded by FCT –under SFRH/BD/140550/2018.

Appendix A. Supplementary data

Supplementary data to this article can be found online at https://doi.org/10.1016/j.cej.2021.130538.

References

[1] M. Karimi, J.A. C. Silva, C.N.d.P. Gonçalves, J. L. Diaz de Tuesta, A.E. Rodrigues, H. T. Gomes, CO_2 capture in chemically and thermally modified activated carbons using breakthrough measurements: experimental and modeling study, Ind. Eng. Chem. Res. 57 (32) (2018) 11154–11166.

[2] M. Karimi, L. Zafanelli, J.P.P. Almeida, G.R. Ströher, A.E. Rodrigues, J.A.C. Silva, Novel insights into activated carbon derived from municipal solid waste for CO_2 uptake: synthesis, adsorption isotherms and scale-up, J. Environ. Chem. Eng. 8 (2020), 104069.

[3] M. Karimi, M.R. Rahimpour, R. Rafiei, M. Jafari, D. Iranshahi, A. Shariati, Reducing environmental problems and increasing saving energy by proposing new configuration for moving bed thermally coupled reactors, J. Nat. Gas Sc. Eng. 17 (2014) 136–150.

[4] B.P. Spigarelli, S.K. Kawatra, Opportunities and challenges in carbon dioxide capture, J. CO_2 Util. 1 (2013) 69–87.

[5] H. Yu, X. Wang, C. Xu, D.-L. Chen, W. Zhu, R. Krishna, Utilizing transient breakthroughs for evaluating the potential of Kureha carbon for CO_2 capture, Chem. Eng. J. 269 (2015) 135–147.

[6] M. Karimi, M.R. Rahimpour, D. Iranshahi, Enhancing BTX production in refineries accompanied with sulfur dioxide oxidation by using new thermal integrated model in fixed bed reactors, Chem. Eng. Technol. 41 (2018) 1746–1758.

[7] P. Bains, P. Psarras, J. Wilcox, CO_2 capture from the industry sector, Prog. Energy Combust. Sci. 63 (2017) 146–172.

[8] A.D.N. Kamkeng, M. Wang, J. Hu, W. Du, F. Qian, Transformation technologies for CO_2 utilisation: Current status, challenges and future prospects, Chem. Eng. J. 409 (2021), 128138.

[9] M. Karimi, A.E. Rodrigues, J.A.C. Silva, Biomass as a source of adsorbents for CO_2 capture, in: M.R. Rahimpour, R. Kamali, M.A. Makarem, M.K.D. Manshadi (Eds.), Advances in Bioenergy and Microfluidic Applications, Amsterdam, Elsevier Pub, 2021, pp. 255–274.

[10] R. Checchetto, G. Trettel, A. Miotello, Sievert-type apparatus for the study of hydrogen storage in solids, Meas. Sci. Technol. 15 (1) (2004) 127–130.

[11] A. Sieverts, Information on the occlusion and diffusion of gases through metals, Z. Phys. Chem. 60 (2) (1907) 129–201.

[12] A.J. Lachawiec, T.R. DiRaimondo, R.T. Yang, A robust volumetric apparatus and method for measuring high pressure hydrogen storage properties of nanostructured materials, Rev. Sci. Instrum. 79 (2008), 063906.

[13] F. Dreisbach, R. Staudt, J.U. Keller, High pressure adsorption data of methane, nitrogen, carbon dioxide and their binary and ternary mixtures on activated carbon, Adsorption 5 (1999) 215–227.

[14] W. Sievers, A. Mersmann, Single and multicomponent adsorption equilibria of carbon dioxide, nitrogen, carbon monoxide and methane in hydrogen purification processes, Chem. Eng. Technol. 17 (1994) 325–337.

[15] K. Munusamy, G. Sethia, D.V. Patil, P.B.S. Rallapalli, R.S. Somani, H.C. Bajaj, Sorption of carbon dioxide, methane, nitrogen and carbon monoxide on MIL-101 (Cr): volumetric measurements and dynamic adsorption studies, Chem. Eng. J. 195–196 (2012) 359–368.

[16] J.A. Mason, T.M. McDonald, T.H. Bae, J.E. Bachman, K. Sumida, J.J. Dutton, S. S. Kaye, J.R. Long, Application of a high-throughput analyzer in evaluating solid adsorbents for post-combustion carbon capture via multicomponent adsorption of CO_2, N_2, and H_2O, J. Am. Chem. Soc. 137 (2015) 4787–4803.

[17] H. CHENG, X. DENG, S. LI, W. CHEN, D. CHEN, K. YANG, Design of PC based high pressure hydrogen absorption/desorption apparatus, Int. J. Hydrogen Energ. 32 (14) (2007) 3046–3053.

[18] A. Policicchio, E. Maccallini, G.N. Kalantzopoulos, U. Cataldi, S. Abate, Volumetric apparatus for hydrogen adsorption and diffusion measurements: Sources of systematic error and impact of their experimental resolutions, Rev. Sci. Instrum. 84 (2013), 103907.

[19] Y. Belmabkhout, M. Frère, G.D. Weireld, High-pressure adsorption measurements. A comparative study of the volumetric and gravimetric methods, Meas. Sci. Technol. 15 (5) (2004) 848–858.

[20] S. Ramaprabhu, N. Rajalakshmi, A. Weiss, Design and development of hydrogen absorption/desorption high pressure apparatus based on the pressure reduction method, Int. J. Hydrogen Energ. 23 (1998) 797–801.

[21] A. Qajar, M. Peer, R. Rajagopalan, H.C. Foley, High pressure hydrogen adsorption apparatus: design and error analysis, Int. J. Hydrogen Energ. 37 (11) (2012) 9123–9136.

[22] S. Sircar, Gibbsian surface excess for gas adsorption. Revisited, Ind. Eng. Chem. Res. 38 (10) (1999) 3670–3682.

[23] O. Talu, Needs, status, techniques and problems with binary gas adsorption experiments, Adv. Colloid Interfac. 76-77 (1998) 227–269.

[24] R. Seabra, A.M. Ribeiro, K. Gleichmann, A.F.P. Ferreira, A.E. Rodrigues, Adsorption equilibrium and kinetics of carbon dioxide, methane and nitrogen on binderless zeolite 4A adsorbents, Micropor. Mesopor. Mat. 277 (2019) 105–114.

[25] M.L. Pavlov, O.S. Travkina, B.I. Kutepov, Grained binder-free zeolites: synthesis and properties, Catal. Ind. 4 (2012) 11–18.

[26] C. Feng, J. E, W. Han, Y. Deng, B. Zhang, X. Zhao, D. Han, Key technology and application analysis of zeolite adsorption for energy storage and heat-mass transfer process: A review, Renew. Sust. Energ. Rev. 144 (2021) 110954.

[27] P. Gabrielli, M. Gazzani, M. Mazzotti, The role of carbon capture and utilization, carbon capture and storage, and biomass to enable a Net-Zero-CO2 emissions chemical industry, Ind. Eng. Chem. Res. 59 (2020) 7033–7045.

[28] D. D'Alessandro, B. Smit, J. Long, Carbon dioxide capture: prospects for new materials, Angew. Chem. Int. Ed. 49 (35) (2010) 6058–6082.

[29] https://www.cwk-bk.de/en/.

[30] A.D. Wiersum, C. Giovannangeli, D. Vincent, E. Bloch, H. Reinsch, N. Stock, J. S. Lee, J.-S. Chang, P.L. Llewellyn, Experimental screening of porous materials for high pressure gas adsorption and evaluation in gas separations: application to MOFs (MIL-100 and CAU-10), ACS Comb. Sci. 15 (2013) 111–119.

[31] S. Sircar, Excess properties and thermodynamics of multicomponent gas adsorption, J. Chem. Soc. Faraday Trans. 81 (1985) 1527–1540.

[32] S. Sircar, Measurement of gibbsian surface excess, AIChE J. 47 (5) (2001) 1169–1176.

[33] S. Sircar, Gibbsian surface excess for gas adsorption revisited, Ind. Eng. Chem. Res. 38 (1999) 3670–3682.

[34] J.U. Keller, R. Staudt, Gas Adsorption Equilibria Experimental Methods and Adsorptive Isotherms, Springer, New York, 2005.

[35] S. Gumma, O. Talu, Gibbs dividing surface and helium adsorption, Adsorption 9 (2003) 17–28.

[36] F.G. Kerry, Industrial Gas Handbook: Gas Separation and Purification, Taylor & Francis Group, Oxfordshire, 2006.

[37] K.Y. Foo, B.H. Hameed, Insights into the modeling of adsorption isotherm systems, Chem. Eng. J. 156 (1) (2010) 2–10.

[38] J.H. De Boer, The Dynamical Character of Adsorption, 2nd ed., Oxford University Press, London, 1968.

[39] A.L. Myers, J.M. Prausnitz, Thermodynamics of mixed gas adsorption, AIChE J. 11 (1) (1965) 121–127.

[40] A. Malek, S. Farooq, Comparison of isotherm models for hydrocarbon adsorption on activated carbon, AIChE J. 42 (11) (1996) 3191–3201.

[41] J.A.C. Silva, K. Schumann, A.E. Rodrigues, Sorption and kinetics of CO_2 and CH_4 in binderless beads of 13X zeolite, Micropor. Mesopor. Mat. 158 (2012) 219–228.

[42] D.D. Do, Adsorption Analysis: Equilibria and Kinetics: (With CD Containing Computer Matlab Programs), World Scientific, 1998.

[43] Y. Park, Y. Ju, D. Park, C.H. Lee, Adsorption equilibria and kinetics of six pure gases on pelletized zeolite 13X up to 1.0 MPa: CO_2, CO, N_2, CH_4, Ar and H_2, Chem. Eng. J. 292 (2016) 348–365.

[44] Y. Park, D.K. Moon, Y.H. Kim, H. Ahn, C.H. Lee, Adsorption isotherms of CO_2, CO, N_2, CH_4, Ar and H_2 on activated carbon and zeolite LiX up to 1.0 MPa, Adsorption 20 (2014) 631–647.

[45] D.M. Ruthven, Principles of Adsorption and Adsorption Processes, 1st ed., John Wiley & Sons, New York, 1984.

[46] S. Sircar, R. Mohr, C. Ristic, M. Rao, Isosteric heat of adsorption: theory and experiment, J. Phys. Chem. B 103 (1999) 6539–6546.

[47] A. Romero-Pérez, G. Aguilar-Armenta, Adsorption kinetics and equilibria of carbon dioxide, ethylene, and ethane on 4A (CECA) zeolite, J. Chem. Eng. Data 55 (9) (2010) 3625–3630.

[48] R.J. Harper, G.R. Stifel, R.B. Anderson, Adsorption of gases on 4A synthetic zeolite, Can. J. Chem. 47 (24) (1969) 4661–4670.

[49] A. Streb, M. Mazzotti, Adsorption for efficient low carbon hydrogen production: part 1-adsorption equilibrium and breakthrough studies for $H_2/CO_2/CH_4$ on zeolite 13X, Adsorption (2021), https://doi.org/10.1007/s10450-021-00306-y.

[50] S. Sircar, Linear-driving-force model for non-isothermal gas adsorption kinetics, J. Chem. SOC, Faraday Trans. I (79) (1983) 785–796.

[51] D.D. Do, R.G. Rice, Validity of the parabolic profile assumption in adsorption studies, AIChE J. 32 (1) (1986) 149–154.

[52] M. Karimi, J.L. Diaz de Tuesta, C.N. d. P. Gonçalves, H.T. Gomes, A.E. Rodrigues, J. A.C. Silva, Compost from municipal solid wastes as a source of biochar for CO_2 capture, Chem. Eng. Technol. 43 (7) (2020) 1336–1349.

[53] S.M. Sidik, S. Triwahyono, A.A. Jalil, Z.A. Majid, N. Salamun, N.B. Talib, T.A. T. Abdullah, CO_2 reforming of CH_4 over Ni–Co/MSN for syngas production: Role of Co as a binder and optimization using RSM, Chem. Eng. J. 295 (2016) 1–10.

[54] S. García, M.V. Gil, C.F. Martín, J.J. Pis, F. Rubiera, C. Pevida, Breakthrough adsorption study of a commercial activated carbon for pre-combustion CO_2 capture, Chem. Eng. J. 171 (2) (2011) 549–556.

[55] A. Henrique, M. Karimi, J.A.C. Silva, A.E. Rodrigues, Analyses of adsorption behavior of CO_2, CH_4, and N_2 on different types of BETA zeolites, Chem. Eng. Technol. 42 (2) (2019) 327–342.

[56] M. Shirzad, M. Karimi, Statistical analysis and optimal design of polymer inclusion membrane for water treatment by Co(II) removal, Desalin. Water Treat. 182 (2020) 194–207.

[57] R.H. Myers, D.C. Montgomery, C.M. Anderson-Cook, Response surface methodology: process and product optimization using designed experiments, 4th ed., Wiley Publication, New Jersey, 2016.

[58] L. Zafanelli, A. Henrique, M. Karimi, A.E. Rodrigues, J.A.C. Silva, Single and multicomponent fixed bed adsorption of CO_2, CH_4, and N_2 in binder-free beads of 4A zeolite, Ind. Eng. Chem. Res. 59 (2020) 13724–13734.

[59] R.M. Barrer, Zeolites and Clay Minerals as Sorbents and Molecular Sieves, VII.; Academic Press, London, 1978.

[60] A. Streb, M. Mazzotti, Adsorption for efficient low carbon hydrogen production: Part 2-Cyclic experiments and model predictions, Adsorption (2021), https://doi.org/10.1007/s10450-021-00308-w.